energies
MDPI

Article

Investigation of the Energy Saving Efficiency of a Natural Ventilation Strategy in a Multistory School Building

Beungyong Park [1] and Sihwan Lee [2,*]

1 Energy Division, Korea Conformity Laboratories (KCL), Jincheon 27872, Korea; bypark@kcl.re.kr or qkqudy@gmail.com
2 Department of Architecture, Shinshu University, 4-17-1 Wakasato, Nagano City 380-8553, Japan
* Correspondence: shany@shinshu-u.ac.jp

Received: 2 March 2020; Accepted: 3 April 2020; Published: 6 April 2020

check for updates

Abstract: Under-ventilation and high energy consumption are some of the problems associated with school classrooms. Thus, it is necessary to develop a ventilation strategy that is characterized by high energy-saving and ventilation efficiency. To this end, this study aims to investigate natural ventilation as a possible strategy to improve the indoor environment while reducing ventilation loads and maintaining energy costs during intermediate seasons. Ventilation and cooling load reductions based on the opening and closing of several windows were analyzed. Window flow coefficients and ventilation rates were measured and used for computational fluid dynamics (CFD) simulation to obtain pressure coefficients for 16 wind directions. The results obtained showed that the improved natural ventilation strategy could be used to effectively establish required indoor conditions (26 °C, 60% RH). Additionally, compared with the mechanical ventilation system with variable refrigerant flow, this natural strategy resulted in a decrease in energy consumption of approximately 30%. However, its application requires that internal heat gain and CO_2 emissions, which depend on human population density, as well as the room usage schedule should be considered.

Keywords: void; natural ventilation; field measurement; CFD; cooling load

1. Introduction

Recently, owing to problems associated with the reduction of energy consumption and greenhouse gas emission, there has been increasing interest in the development of energy-saving systems and environmentally friendly building methods. Particularly, many studies on indoor environmental control using natural environmental control approaches are being conducted around the world.

In the building construction industry, to maintain a comfortable indoor environment and provide a better indoor air quality (IAQ), building ventilation is one of the most important parameters that is taken into consideration. School classroom under-ventilation and high energy consumption have been reported in the literature. For example, Montazami et al. [1] reported that aircraft noise, overheating, and poor air quality are some of the problems associated with classrooms in London. Their study established that overheating could be managed via ventilation control. Additionally, Mendell and Heath [2] reported that a low ventilation rate in classrooms, coupled with poor air quality resulted in a significant decrease in learning performance.

To maintain a comfortable environment and a pleasant atmosphere for learning, mechanical ventilation systems are commonly installed to provide fresh air. However, this leads to high energy consumption; thus, there is need for the development of a ventilation strategy that ensures better energy saving and high-efficiency ventilation. Natural ventilation, which can be properly controlled based on changes in external environmental conditions, is a passive technology that can be employed to improve the indoor environment, while reducing ventilation loads and maintenance energy costs during intermediate seasons.

To understand the mechanism of natural ventilation, an analysis of air movement inside and outside buildings is required. Additionally, natural ventilation is classified as pressure differential ventilation, which is based on external wind velocity as well as internal and external pressure differentials, and temperature differential ventilation, which is based on internal and external temperature differentials. In 1926, Emswiler [3] proposed a basic theory of natural convection (air movement) through openings in fluids of different densities, and based on his theory, various tools, such as TRNSYS 17 (Madison, USA), in combination with air CONTAM(Maryland, USA), air flow network programs, and computer fluid dynamics (CFD) models, are being used today to simulate natural ventilation [4]. Natural ventilation analysis depends on external conditions, and several studies have established boundary conditions for natural ventilation using test chambers [5] or wind tunnel model experiments [6]. However, investigating the natural ventilation of actual buildings using these existing methods remains challenging.

Several studies have been conducted to investigate the factors that influence natural ventilation using the abovementioned tools. In this regard, to investigate natural ventilation systems in combination with operable windows, the influence of operable windows or ventilation openings in buildings has been examined [7,8]. Shetabivash [9] reported that natural ventilation can be influenced by the shape, size, and location of the openings, and based on the results of wind tunnel experiments, Ji et al. [10] reported that instantaneous fluctuations in wind direction and wind speed also influence natural ventilation. Additionally, wind pressure coefficients (C_p) are influenced by a wide range of parameters, including building geometry, topographic location of a building site, façade detailing, façade position, the degree of exposure/sheltering, wind speed, and wind direction. Karava et al. [11] investigated the effect of wall porosity and opening location on ventilation flow rates using wind tunnel measurements. The test model for opening configurations that they considered was designed to evaluate wind-driven cross-ventilation in a single zone with two openings. Their results showed that the inlet-to-outlet ratio and façade location on a building are important parameters to consider in the evaluation of air flow in buildings with cross-ventilation.

Gough [12] measured the change in natural ventilation under actual atmospheric conditions using tracer gas and pressure-based methods. To verify the accuracy of the two measurement methods based on the external wind environment, cubic buildings of the same size were used, thus, it was possible to estimate the true ventilation rate as a function of wind speed.

Design guidelines are also offered in building regulations other literature and include a variety of recommendations [13,14].

However, to control the adequate natural ventilation rate for a room is still challenging, owing to many uncertain factors, including, wind pressure on building façades, variable wind speeds and directions, the presence of internal and external openings, the location of the openings and their size, and variations in outdoor temperature from time to time. Natural ventilation control strategies have been analyzed theoretically, and the practical applicability of the results of these analyses is limited. Thus, to improve ventilation control in actual buildings, it is necessary to examine actual natural ventilation characteristics.

Thus, the purpose of this study was to adequately investigate natural ventilation strategies so as to enhance natural ventilation in green building designed actual building. To maximize the cross-ventilation effect as well as the mechanism of general mechanical ventilation and air conditioning, the effectiveness of the natural ventilation control strategy was verified by comparing and analyzing the ventilation and cooling load reductions based on the opening and closing of several windows. The flow coefficient of each window was analyzed using the natural ventilation measurements based on each open window. To overcome the limitations associated with the experiments, numerical evaluation methods based on CFD simulation that have been applied in several other studies, were used to determination of wind C_p based on the external environment of the building (the measured wind velocity). The energy load was calculated via network simulations using the flow coefficients and the C_p. Regarding design strategies, this study focused on the provision of voids, i.e., air wells or atria, which are usually placed in the center of buildings, and represent a passive architectural feature that is adopted for natural ventilation.

2. Materials and Methods

In this study, measurements and simulations were used to examine the effect of natural ventilation control on energy load by opening and closing ventilation ports that reflected the effective area of the openings on the target building.

Figure 1 shows the analysis flow that was employed in this study. Firstly, to determine flow coefficients and ventilation rates as a function of pressure differences, the natural ventilation rates, window flow coefficients, and weather data for the multistory school building were measured. Secondly, to model the outdoor wind environment and evaluate the C_p, CFD simulation was used to calculate C_p for 16 wind directions. Thereafter, the wind C_p at the windows and at the void exits was analyzed.

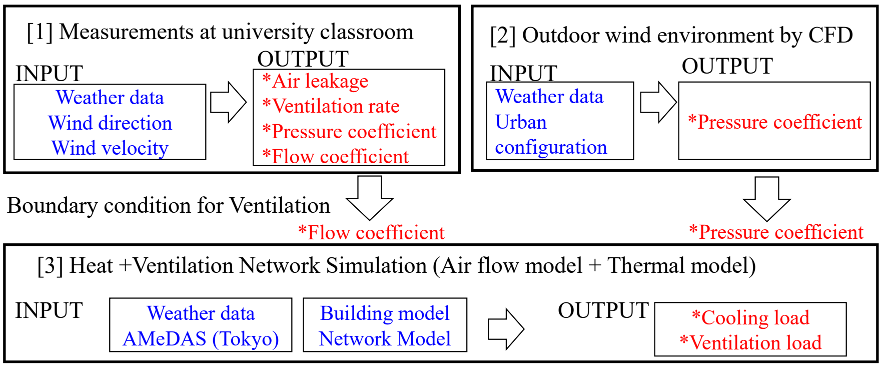

Figure 1. Analysis flow.

Flow coefficients and C_p measurements represent the most common secondary data source for heat and ventilation network simulations using TRNSYS with TRNFLOW for the evaluation of the cooling effect of the natural ventilation strategy during intermediate seasons [15].

Finally, thermal network simulations were performed using the effective area of the openings of the building, and the wind C_p of the exterior were used to calculate the changes in the ventilation volume of the room with time. Thus, the cooling and ventilation loads of the intermediate and summer seasons were calculated.

2.1. Field Measurements

In this study, the relationship between differential pressure and natural ventilation rate was analyzed, and field measurements were conducted in a medium rise multi-story school building located in Tokyo, Japan (35.7 N; 139.8 E). The building, which was constructed in February, 2013, consists of eleven stories, and is used as a university laboratory. It has a total floor area of 4,453,797 m^2 as shown in Figure 2a,b shows the floor plan of the sixth floor, while Figure 2c shows the room that was targeted for the field measurements, as well as the measurement points.

Figure 3 shows the sliding windows (1800 mm × 1575 mm), the top hung window (1240 mm × 300 mm), the top hung window at the void side (2270 mm × 930 mm), and the door (800 mm × 300 mm) of the target room located (volume = 6.6 m (x) × 9.3 m (y) × 2.3 m (z), floor area = 155 m^3). Table 1 presents the details of the measured quantities.

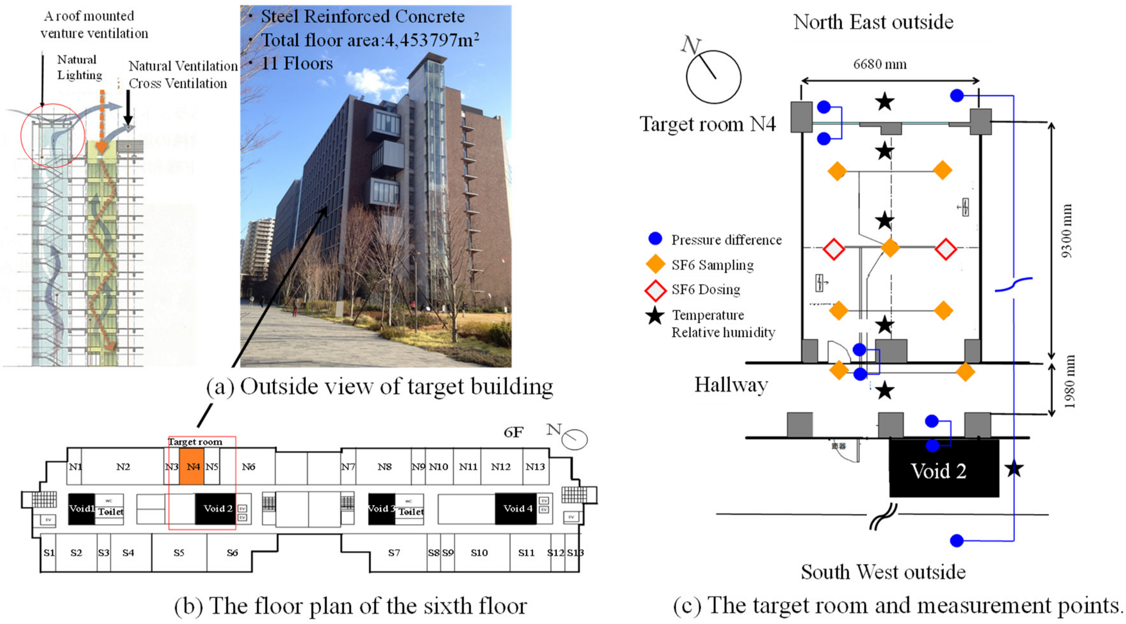

Figure 2. Schematic representation of the target building and measurement points: (**a**) outside view of target building; (**b**) the floor plan of the sixth floor and (**c**) the target room and measurement points.

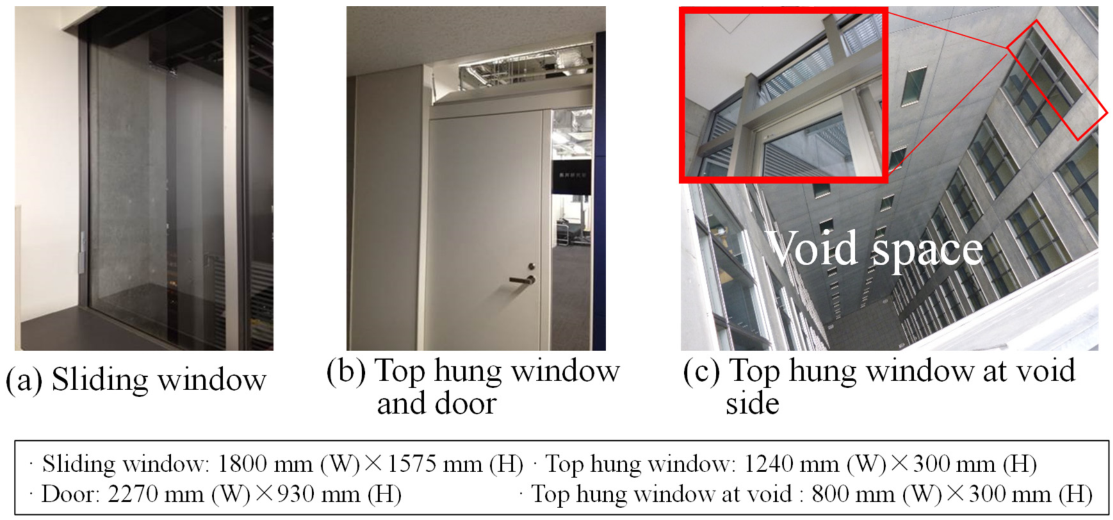

Figure 3. Schematic representation of the target building windows and door: (**a**) sliding window; (**b**) top hung window and door and (**c**) top hung window at void side.

Table 1. Details of the measured items.

Items	Method	Device
Infiltration	Tracer gas measurement (decay method).	Multi-gas monitor type 1302 (B&K) Multipoint sampler type 1303 (B&K) SF_6 gas
Ventilation rate	Tracer gas measurement (constant concentration method).	
Difference pressure	Difference pressure meter	SETRA model 239 (±1% at 20 °C DB).
Wind data	Acoustic resonance principle	PFWS-100 (0–60 m/s, (±0.2%)).
Temperature and humidity	Temperature and humidity sensor (type-t thermal couple)	TR-503 (0–55 °C (±0.3 °C)); –95% R.H. (± 5% R.H.); Diameter = 0.5 mm.

The airflow performances of the sliding window, the top-hung door opening, and the void were also calculated based on measurements of the room's airflow characteristics with the ventilator open and closed. The natural ventilation rate was measured using the tracer gas test method, and the pressure differential was measured at various applied pressures during the intermediate season (between August 25 and October 21, 2015). The airflow performance of the ventilator was calculated at across opening, and it was typically described by its flow coefficient, which is defined according to Equation (1).

$$Q = \alpha A \sqrt{\frac{2\Delta P}{\rho}} \quad (1)$$

where, Q (m^3/h), α (-), A (m^2), ΔP (Pa), and ρ (kg/m^3) represent ventilation rate, flow coefficient, area of opening, pressure difference across opening, and air density, respectively.

To collect data on wind direction, wind speed, and differential pressure at intervals of 1 min, an anemometer was set up at the center of the roof ridge of the target building (52 m above ground level).

2.2. CFD Simulation Methods

Figure 4 shows the geometry of the configuration of the building for CFD simulations, while Figure 5 shows the analysis of the wind C_p for 16 wind directions using CFD simulation. Table 2 summarizes the calculation conditions.

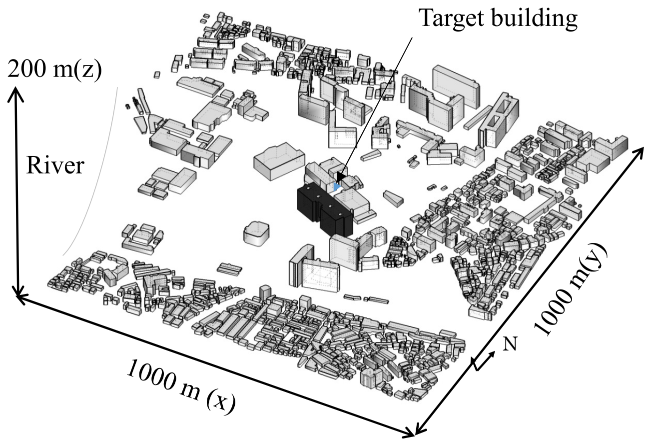

Figure 4. Geometry of the building configurations for computational fluid dynamics (CFD) simulations.

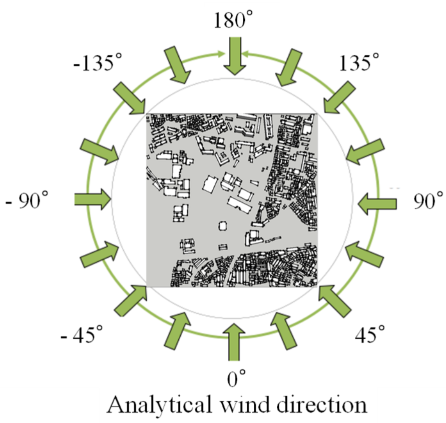

Figure 5. Analysis of cases for wind pressure coefficients for 16 wind directions.

Table 2. Summary of calculation conditions.

Items	Specifications
Turbulent Model	SST k-ω model (STAR-CD ver.4.2)
Mesh	994,591 Trimmed mesh (hexahedral)
Boundary conditions	1000 (x) × 1000 (y) × 200 (z) m, $U = U_0\ (Z/Z_0)^{0.25}$, $U_0 = 1$ m/s, $Z_0 = 52$ m
Difference scheme	Convection term: 1st order upwind, Diffusion term: central difference

The building and its surroundings were reproduced within a 1000 m radius from the target building. The geometry of most of the buildings within this 1000 m radius included low-rise houses, high-rise buildings, commercial facilities, and single-family houses. The conditions surrounding the target building were determined using maps from Google Earth as well as on-site investigations. Building height data was obtained from solar radiation diagrams, and a city block model was developed using Google SketchUp ver.8.0 (California, USA), and by using Star-CD ver.4.2 (Newyork, USA), it was possible to develop a city block model over an auto-mesh.

The wind pressure enveloping a building is usually expressed as pressure coefficients (C_p), which are defined by Equation (2) below.

$$C_p = \frac{P_x - P_0}{P_d} \tag{2}$$

$$P_d = \frac{\rho \times {V_h}^2}{2} \tag{3}$$

where P_x (Pa), P_0 (Pa), P_d (Pa), and V_h (m/s) represent the static pressure at a given point on the building façade, the static reference pressure, the dynamic pressure, and the wind speed (often considered at building height, h (m) in the upstream undisturbed flow), respectively [1].

2.3. Heat and Ventilation Network Simulation Methods

In this study, energy saving in buildings via the improvement of the natural ventilation strategy was attempted. Thus, TRNSYS simulation with the TRNFLOW network was used. For the purpose of simulation, given that the building consists of classrooms, hallways, staircases, and voids, the building model was simplified, and the complexity of the relationship between building heights in this model was reduced. Figure 6 shows a simplified building model and the plan of the network simulation in the buildings. Figure 7 shows a description of the control strategies for natural ventilation. The weather data used the automated meteorological data acquisition system data (AMeDAS, Japan) based on the 2000-years base. AMeDAS developed by Japan Meteorological Agency, included solar radiation, temperature, humidity, wind velocity, and wind direction. AMeDAS data is the value converted to 6.5 m above the ground. The network simulation was calculated the wind speed for each height by Equation (4).

$$V_h = \left(\frac{h}{6.5}\right)^{\frac{1}{4}} \times V_{6.5} \tag{4}$$

where V_h (m/s) and $V_{6.5}$ (m/s) represent the wind speed at a given point (h (m) is at building height (2 m, 10 m, 22 m, 34 m, 42 m, and 46 m) and 6.5 is the standard measuring height of the AMeDAS weather observation system), respectively [16].

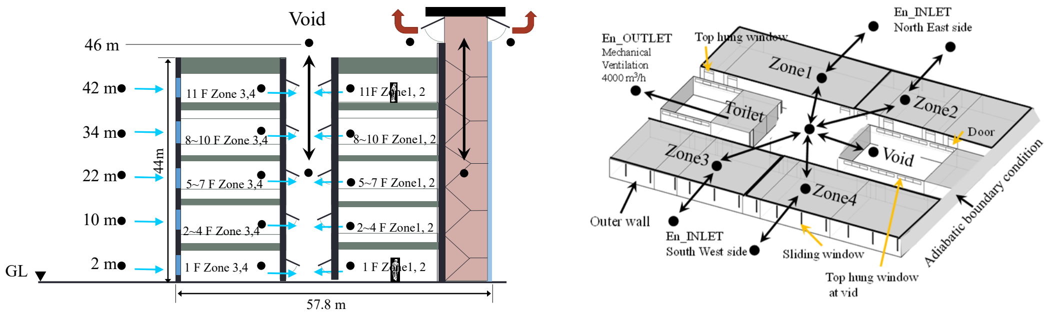

(**a**) The connect of air node in the entire building (**b**) The specification of the floor air node

Figure 6. Simplified building model and the plan of the network simulation in the buildings: (**a**) the connect of air node in the entire building; (**b**) the specification of the floor air node.

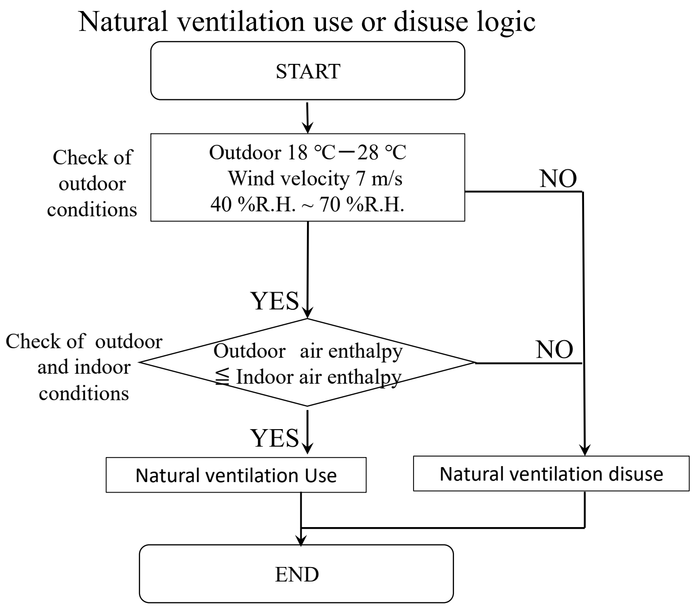

Figure 7. Description of the control strategies for natural ventilation.

The detailed simulation conditions and building details are listed in Table 3. The ventilation rates required for the school classroom were determined based on the Society of Heating, Air-Conditioning, and Sanitary Engineers (SHASE) standard for a half of the maximum expected occupancy profile and the area of the corresponding zone [17]. The indoor air temperature and relative humidity (RH) were specified based on American Society of Heating, Refrigeration and Air-Conditioning Engineers (ASHRAE) comfort ranges [18]. A variable refrigerant flow (VRF) air conditioning system with a heat exchanger ventilation system was installed. It was designed to cover the maximum possible pollution load and heating/cooling loads from persons as well as internal heat and solar gains in the school.

Table 3. Simulation condition and building details.

Items	Specifications
Target model	Area = 2,154,240 m^2; Room height = 2.6 m
Control condition	Set temperature = 26 °C Set humidity = 60% RH (0.0126 kg/kg (DA))
Operation schedule	Operating schedule = Weekdays: 08–23 h
Weather data	AMeDAS weather data, Tokyo, Japan (2000-year based).
U-value	Outer wall = 0.657 W/m^2 K Internal wall = 0.336 W/m^2 K Floor and ceiling = 0.784 W/m^2 K Sliding window = 5.68 W/m^2 K, 15% frame (U = 8.17 W/m^2 K) 1.5 × 0.1 m^2 Top hung window = 0.8 × 0.3 m^2 Top hung void window = 2.4 × 0.4 m^2 Door = 0.8 × 2.1 m^2 Staircase window = 0.9 × 1.6 m^2
Population Density	0.41 (per person/m^2) × 0.5 Set at 50% of the design value in school classroom construction.
Air change rate	20 (m^3/h per person) × population density (per person/m^2) × classroom area (m^2) Toilet = 4000 m^3/h each.
Internal load	Light = 12 W/m^2 (Weekdays: 08–23 h) Per Person = Sensible heat 75 W, Latent heat 75 W (Weekdays: 08–23 h) Computer = 41 W/m^2 (Everyday: 00–23 h) The number of computers is equal to the population density.
Air conditioning (VRF)	Coefficient of performance = 3.5
Mechanical ventilation (Heat exchanger [16])	Heat exchange coefficient = Total 65%, Sensible 70%. Air flow rate = 500 m^3/h Electric consumption = 220 W

Table 4 presents the cases that were analyzed using network simulations for the determination of the natural ventilation rate. The natural ventilation load was characterized with the windows opened and closed.

Table 4. Network simulation analysis cases for natural ventilation rate.

Cases	Sliding Window	Top Hung Window	Top Hung Window at Void Side	Staircase Window
Case 1	Open	Open	Close	Close
Case 2	Open	Open	Open	Close
Case 3	Open	Open	Close	Open
Case 4	Open	Open	Open	Open

The VRF air conditioning system controls indoor temperature and relative humidity for set conditions. In Case 1, the sliding and the top-hung windows were open, and in Case 2, the sliding window, top-hung window, and top-hung window void were opened. In Case 3, the sliding window, top-hung window, and wind-capture window at the staircase where opened, and in Case 4, the sliding window, top-hung window, top-hung window void, and wind-capture window at the staircase were open. Heat demand was calculated such that the total sensible and latent loads were simulated within the energy requirements for indoor air temperature and relative humidity.

The improved natural ventilation strategy was as follows. Natural ventilation only was used when the outside air conditions were favorable based on indoor and outdoor enthalpies. The required outdoor airflow rate determined based on the population density and occupancy schedule of the building was considered as the natural ventilation rate. The windows were opened or closed depending on the required ventilation rates, defined according to Equation (5).

$$Q = \frac{M \times 100}{C_t - C_0} \quad (5)$$

where Q (m^3/h per person), M (m^3/h), C_t (ppm), and C_0 (ppm) represent the outdoor airflow rate required per person, the CO_2 emission rate per person (0.022 m^3/h), the maximum CO_2 concentration (1500 ppm), and the outdoor base CO_2 concentration (400 ppm), respectively. Here, Q was calculated 20 m^3/h per person.

3. Results and Discussions

3.1. Results of Measurement

Figure 8 shows the change in natural ventilation as a function of the differential pressure and wind speed. Particularly, Figure 8a shows the change in natural ventilation with differential pressure. Natural ventilation was calculated using the differential pressures resulting from the opening and closing of the windows, and at the north-east and void side. Even at low differential pressures, large openings, i.e., the sliding window, the top hung window, and the top hung window at the void side, could bring about significant natural ventilation owing to the cross ventilation effect of the building.

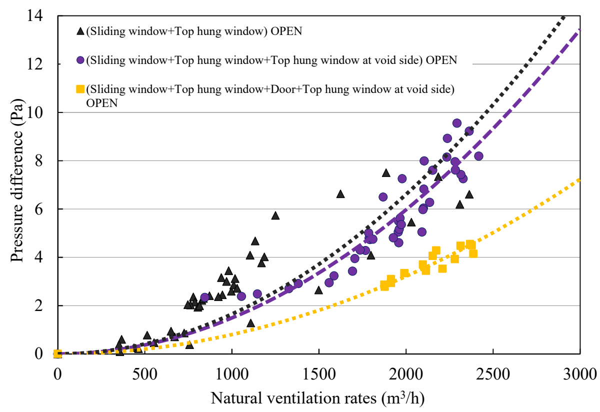

(**a**)

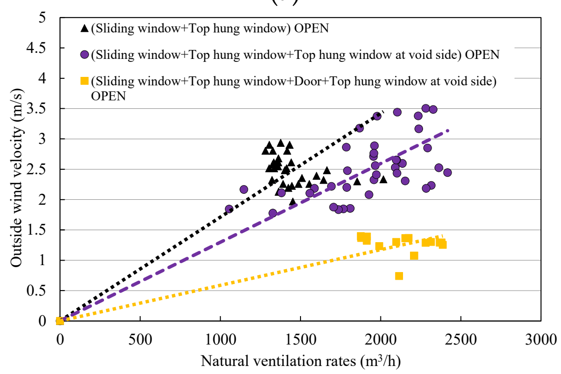

(**b**)

Figure 8. Measurement results of natural ventilation rates: (**a**) change in natural ventilation with differential pressure and (**b**) change in natural ventilation with external wind velocity.

Figure 8b shows the change in natural ventilation with external wind velocity based on the analysis of the data collected using a wind velocity sensor that was placed on the roof of the target building and the natural ventilation results obtained from the differential pressure measurement in shown in Figure 8a. When the large opening was opened, it was confirmed that natural ventilation ≥ 2000 m^3/h occurred even at an external wind speed ranging between 1.0 and 1.5 m/s. The relation between the differential pressure and the natural ventilation rate when using the sliding window or the top-hung window, or both, was analyzed, and the results obtained for the flow coefficient measurements are presented in Table 5. The sliding window flow coefficient was 0.71. That of the top-hung window was 0.74, while that of the top-hung void window was 0.70. A flow coefficient of 0.5 was used for the staircase window [7]. These flow coefficients were used as the boundary conditions for the TRNFLOW network.

Table 5. Analysis case for natural ventilation rate network simulation.

Items	Sliding Window	Top Hung Window	Top Hung Window at Void Side
Flow coefficient (-)	α = 0.71	α = 0.74	α = 0.70

* A flow coefficient of 0.5 was used for the staircase window.

3.2. *Result of Pressure Coefficient of CFD Simulation*

Figure 9 shows the result of the analysis of the pressure coefficients of four wind directions. Positive and negative C_p are shown according to the wind direction of the north and south sides of the sixth floor of the target building. The average C_p of the building façade was used in the TRNFLOW network as the boundary conditions.

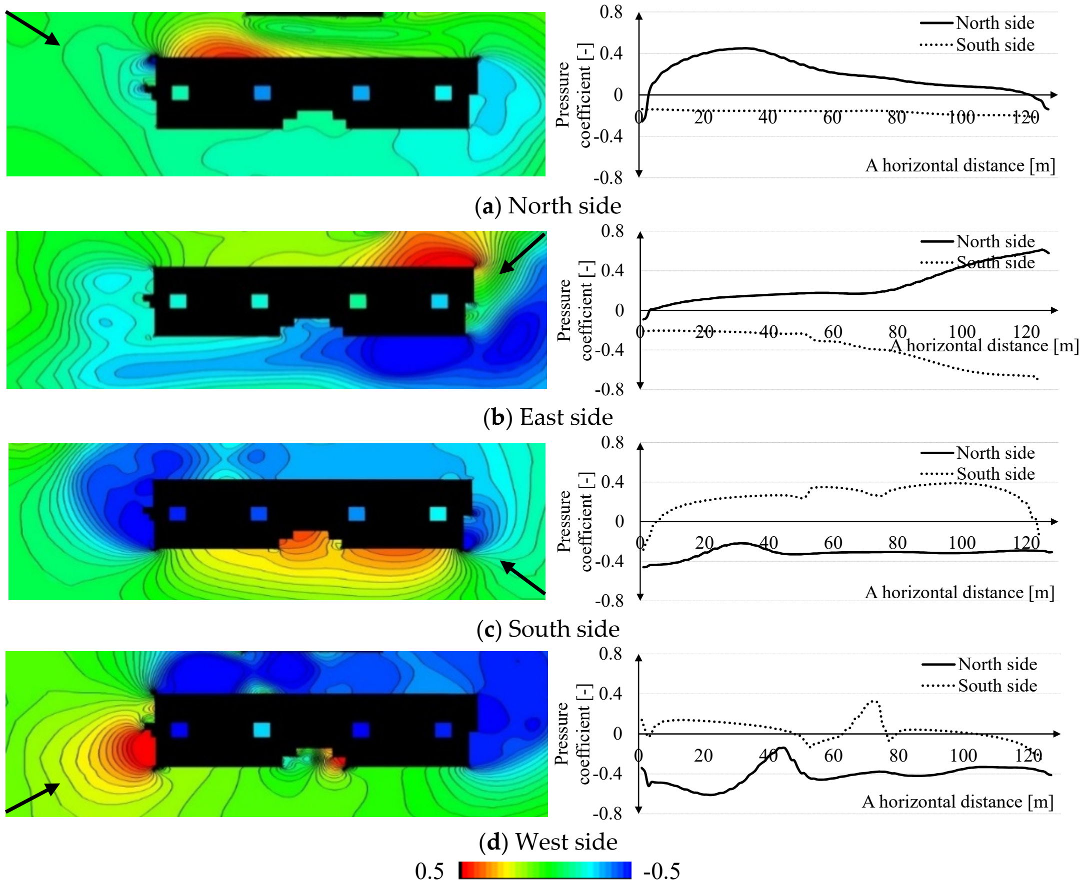

Figure 9. Description of the control strategies for natural ventilation: (**a**) north; (**b**) east; (**c**) south; and (**d**) west sides.

3.3. Discussion on Cooling and Ventilation Demand

The mean monthly temperature and humidity ratio in Tokyo are shown in Figure 10. The weather data was obtained from AMeDAS. Comparisons of the monthly mechanical ventilation variable air volume (VAV) heat demand with the VAV heat demand of natural ventilation are shown in Figure 11. The windows were opened or closed depending on the required ventilation rates under the control strategies for natural ventilation. There was a decrease in the sensible heat demand when the air volume was increased by opening the voids (Cases 2 and 4). Particularly, in Case 2, there was a decrease of 18% in the annual natural ventilation VAV head demand compared with that of the mechanical ventilation system (heat exchanger). This decrease in VAV heat demand resulting from the natural ventilation indicates that VAV could be controlled to establish required indoor conditions (26 °C, 60% RH). Figure 12 showed the electric power consumption of VAV and mechanical ventilation fans. In a future study, a detailed analysis of the effect of the stack effect (Case 4) due to the use of the staircase window will be conducted.

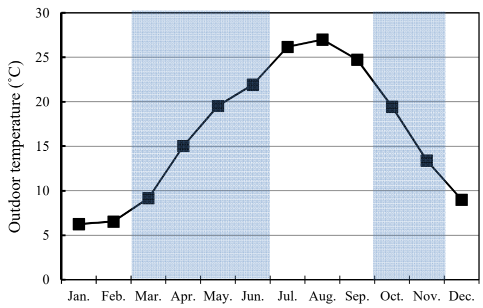

(**a**)

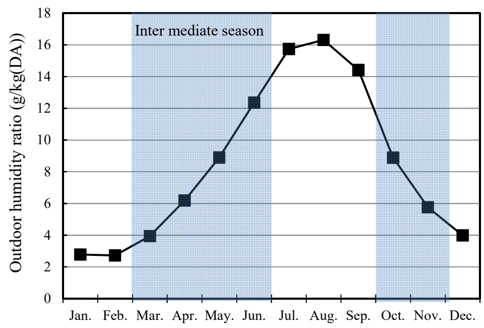

(**b**)

Figure 10. Average monthly outdoor air temperature and humidity ratio (obtained from the automated meteorological data acquisition system data (AMeDAS), Tokyo, Japan): (**a**) outdoor air temperature and (**b**) outdoor air humidity ratio.

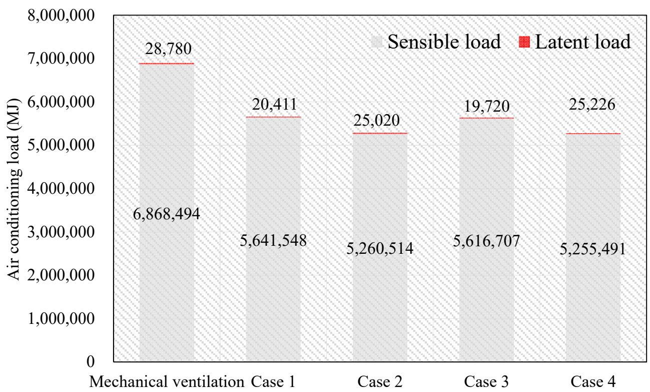

Figure 11. Energy load demand for the target variable air volume (VAV) environment based on comparisons between mechanical ventilation and window opening (natural ventilation).

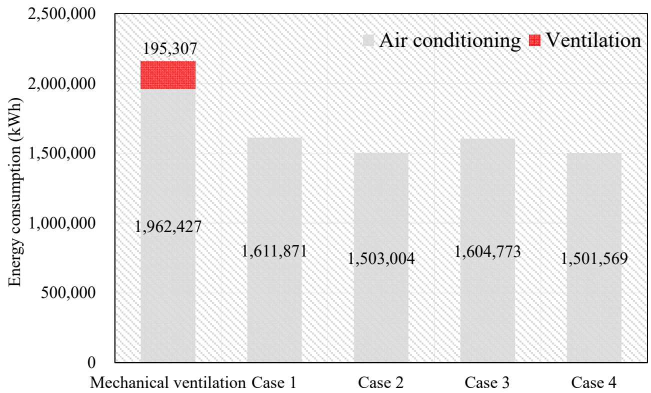

Figure 12. Electric power consumption of VAV and mechanical ventilation fans. The VAV C_p value was 3.5, the sensible and latent loads were the same, and the electric power consumption of the heat exchanger was 220 W (the number of hours of use per day was 15 h/day (137 days)/ 120 Ea).

4. Conclusions

In this study, an improved natural ventilation strategy that is comparable with mechanical ventilation (heat exchanger system) was designed. The effective area of different openings, and their shapes made the evaluation of two ventilation rate measurement methods (i.e., wind speed and pressure measurements) across a wide range of conditions possible, and the pressure coefficients (C_p) for 16 wind directions were determined using CFD.

The energy performance of the natural ventilation strategy of a building in Japan as well as that of its mechanical ventilation system, were simulated using TRNSYS with a TRNFLOW network. The results obtained showed that the improved natural ventilation strategy effectively reduced energy consumption, and compared with the mechanical ventilation system with VRF, a decrease in energy consumption of approximately 30% was obtained.

The potential for the application of this approach to building operation still needs further investigation. Additionally, its application requires that internal heat gain and CO_2 emissions, which depend on human population density, as well as the room usage schedule, should be considered.

Author Contributions: All the authors contributed equally in the preparation of this manuscript. All authors have read and agreed to the published version of the manuscript.

Funding: This work was supported by the National Research Foundation of Korea (NRF) grant funded by the Korea government (MSIT, MOE) and (No. 2019M3E7A1113092). ※ MSIT: Ministry of Science and ICT, MOE: Ministry of Education.

Acknowledgments: We would like to express our deepest gratitude to Prof. Kurabuchi Takashi and Prof. Nagai Tatsuo from Tokyo University of Science for their contribution to taking measurements and performing simulation calculations. This study was implemented based on a research agreement with Tokyo University of Science.

Conflicts of Interest: The authors declare that no conflict of interest associated with this manuscript.

References

1. Montazami, A.; Wilson, M.; Fergus, N. Aircraft noise, overheating and poor air quality in classrooms in London primary Schools. *Build. Environ.* **2012**, *52*, 129–141. [CrossRef]
2. Mendell, M.; Heath, G. Do indoor pollutants and thermal conditions in schools influence student performance; a critical review of the literature. *Indoor Air* **2005**, *15*, 27–52. [CrossRef] [PubMed]
3. Edward, E.J.; Randall, W.C. The neutral zone in ventilation, TRANS. *Am. Soc. Heat. Vent. Eng.* **1926**, *32*, 59–74.
4. Mateus, N.M.; Simões, G.N.; Lúcio, C.; da Graça, G.C. Comparison of measured and simulated performance of natural displacement ventilation systems for classrooms. *Energy Build.* **2016**, *133*, 185–196. [CrossRef]

5. Stavrakakis, G.M.; Koukou, M.K.; Vrachopoulos, M.G.; Markatos, N.C. Natural cross-ventilation in buildings: Building-scale experiments, numerical simulation and thermal comfort evaluation. *Energy Build.* **2008**, *40*, 1666–1681. [CrossRef]
6. Murakami, S. Wind tunnel test on velocity pressure field of cross-ventilation with open windows. *ASHRAE Trans.* **1991**, *97*, 525–538.
7. Chen, Q. Ventilation performance prediction for buildings: A method overview and recent applications. *Build. Environ.* **2009**, *44*, 848–858. [CrossRef]
8. Cóstola, D.; Blocken, B.; Hensen, J.L.M. Overview of pressure coefficient data in building energy simulation and airflow network programs. *Build. Environ.* **2009**, *44*, 2027–2036. [CrossRef]
9. Shetabivash, H. Investigation of opening position and shape on the natural cross ventilation. *Energy Build.* **2015**, *93*, 1–15. [CrossRef]
10. Ji, L.; Tan, H.; Kato, S.; Bu, Z.; Takahashi, T. Wind tunnel investigation on influence of fluctuating wind direction on cross natural ventilation. *Build. Environ.* **2011**, *46*, 2490–2499. [CrossRef]
11. Karava, P.; Stathopoulos, T.; Athienitis, A.K. Airflow assessment in cross-ventilated buildings with operable façade elements. *Build. Environ.* **2011**, *46*, 266–279. [CrossRef]
12. Gougha, H.L.; Luob, Z.; Haliosa, C.H.; Kingc, M.-F.; Noakesc, C.J.; Grimmonda, C.S.B.; Barlowa, J.F.; Hoxeyd, R.; Quinnd, A.D. Field measurement of natural ventilation rate in an idealised full-scale building located in a staggered urban array: Comparison between tracer gas and pressure-based methods. *Build. Environ.* **2018**, *137*, 246–256. [CrossRef]
13. ASHRAE. *ASHRAE Handbook-Fundamentals, Chapter 26 A Good Discussion of Natural Ventilation Equations and A Basic Source for the Contemporary Practice of Fan-Forced Ventilation*; American Society of Heating, Refrigeration and Air-Conditioning Engineers (ASHRAE): Atlanta, GA, USA, 2007.
14. Liddament, M.W. *A Guide to Energy Efficient Ventilation*; Air Infiltration Ventilation Centre, EU: Coventry, UK, 1996.
15. Akasaka, H.; Nimiya, H.; Soga, K.; Matsumoto, S.I. Development of expanded AMeDAS weather data for building energy calculation in Japan/Discussion. *ASHRAE Trans.* **2000**, *106*, 455.
16. The Society of Heating, Air-Conditioning, and Sanitary Engineers of Japan (SHASE). *Handbook of Fundamentals*; SHASE: Tokyo, Japan, 2009; pp. 449–450.
17. ANSI/ASHRAE. *ANSI/ASHRAE Standard 62.1, Ventilation for Acceptable Indoor Air Quality*; American Society of Heating, Refrigerating and Air-Conditioning Engineers, Inc.: Atlanta, GA, USA, 2007.
18. Available online: http://wwwl7.mitsubishielectric.co.jp/wink/FAN_SN/bfs-150ssu3_1_sn.pdf (accessed on 2 October 2011).